[Article ID] 1003 - 6326(2000)04 - 0435 - 06

Mechanical properties of rapidly solidified Al-Ti alloys after thermal exposure①

WU Jin-ming(吴进明)[1], ZHENG Shi-lie(郑史烈)[1], YUAN Jun(袁 俊)[2], LI Zhi-zhang(李志章)[1], ZENG Yue-wu(曾跃武)[1], JI Zhen-guo(季振国)[2]
(1. Department of Materials Science and Engineering, Zhejiang University, Hangzhou 310027, P.R.China;
2. State Key Laboratory of Silicon Materials, Zhejiang University, Hangzhou 310027, P.R.China)

[Abstract] Mechanical properties, for example the elastic modulus, yield stress and ultimate tensile stress, of the rapidly solidified (RS) Al-Ti alloy after thermal exposure have been investigated using an Instron tensile test machine at a strain rate of $1.5 \times 10^{-4} s^{-1}$. The results show that the elastic modulus of the Al-Ti alloy increases with increasing Ti concentration, which can be predicted with Halpin-Tsai equation, Eshelby method and hereby re-modified shear lag model; the yield strength and the ultimate tensile stress increase with increasing volume fraction and decreasing particle size of the Al_3Ti and fine grain strengthening is suggested to be the main operative strengthening mechanism.

[Key words] Al-Ti alloy; grain strengthening; elastic modulus; mechanical properties
[CLC number] TG135⁺.2 [Document code] A

1 INTRODUCTION

Aluminium alloys reinforced with aluminide particles ($NiAl_3$, $FeAl_3$, $ZrAl_3$, $TiAl_3$, etc) possess high specific strength, high specific modulus and excellent properties both at ambient and elevated temperature[1~6]. Compared with most other aluminium-rich intermetallic, Al_3Ti is very attractive because of its low density ($\rho = 3.3\ g/cm^3$)[4], high melting point (1 350 ℃) and high elastic modulus (220 GPa)[7]. Therefore, Al-Ti alloys have received a considerable amount of attention in recent years.

The morphology of the aciculate $TiAl_3$ in casting Al-Ti alloys is detrimental to the mechanical properties[8]. As a result, rapid solidification (RS) and mechanical alloying (MA) have been explored to produce Al-Ti alloys reinforced with 0.1 ~ 0.5 μm equiaxed $TiAl_3$ particles, and excellent mechanical properties both at ambient temperature and elevated temperature of the alloy have been achieved[2~6,8]. Several strengthening mechanisms, such as the Orowan strengthening, grain strengthening, quenching strengthening and load-sharing effects of particles have been suggested to explain the improved strength of the alloy[2~6]. However, no attention has been paid to the Al-Ti alloy reinforced with $TiAl_3$ particles about several micra. Furthermore, for composites reinforced with particles larger than 1 μm, certain strengthening mechanisms such as the Orowan strengthening are negligible. Also, the retarding effect of the reinforcement on the recrystallization of the matrix changes to the stimulating one, i.e. particle stimulated nucleation (PSN) and hence affects the predominant strengthening mechanism of the composite.

Therefore, it is also of theoretical interests to investigate the strengthening mechanisms of Al-Ti alloys with Al_3Ti size particles range from one to several micra. In this paper, mechanical properties, especially the elastic modulus, which is of engineering interests but has never been investigated thoroughly, of the RS Al-Ti alloy after thermal exposure have been studied.

2 EXPERIMENTAL

Al-1.5Ti, Al-3.5T and Al-10Ti (mass fraction, %) alloy bars with rectangular sections of 20 mm × 10 mm were prepared by rapidly solidification. Details of the method have been described elsewhere[9]. To obtain Al_3Ti particles larger than 1 μm, the bars were thermal exposed at two different conditions: 600 ℃ for 100 h, and 600 ℃ for 100 h + 630 ℃ for 150 h. After removing the pure aluminum jackets, these bars were cold rolled to a thickness of 1.0 mm and then annealed at 500 ℃ for 1 h. All the specimens used in this experiment were treated with this process. To be concise, only the thermal exposure condition will be mentioned in the following.

Microstructures of the alloy were examined by optical microscopy (OM), scanning electron microscopy (SEM) and transmission electron mi-

① [Received date] 1999 - 10 - 03; [Accepted date] 1999 - 12 - 08

croscopy (TEM). Energy dispersive spectrometry (EDS) analysis was conducted to determine Ti concentration of the matrix. Particle size and volume fraction of the alloy were measured with help of a computer-aided image analysis system.

The tensile specimens with a gauge of 33 mm × 10 mm × 1.0 mm were machined from the cold rolled and subsequently annealed plates by spark eroding. The tests were conducted using an Instron tensile test machine at a strain rate of about $1.5 \times 10^{-4} s^{-1}$. Using the tensile stress-strain data obtained from specimens mounted with strain gage, the elastic modulus of the alloy after thermal exposure at 600 ℃ for 100 h was calculated. The fracture surface of the alloy was examined with SEM.

3 RESULTS AND DISCUSSION

3.1 Coarsening of Al_3Ti particles

Table 1 shows some characteristics of structure of the prepared material. The typical metallography in Fig.1 indicates that equiaxed Al_3Ti particles were distributed homogeneously in a matrix of the Al(Ti) solid solution, in which the mass fraction of the soluble Ti kept almost constant with increasing nominal Ti concentration of the alloy. The extended solid solution of 1.3 % ~ 1.6 % Ti in Al is a characteristic of the RS method. It is found that volume fraction of the particle was given obviously by the alloy composition. For a given alloy, nearly the same particle volume fraction was measured after each thermal exposure. The particle size grew slowly from 0.6 μm of as-hot-extruded to 1.6 ~ 2.8 μm after thermal exposure and increased with increasing the Ti concentration. Fig.1(a) indicates that the grain size of Al-1.5 Ti alloy is about 15 ~ 20 μm.

Table 1 Structure characteristics of prepared material

Sample	w(Ti)/ % (1)	φ_c/ % (1)	φ_e/ % (1)	d/μm (1)	d/μm (2)
Al-1.5 Ti	1.3	0.16	0.1	1.6	1.9
Al-3.5 Ti	1.5	4.44	5	1.8	2.3
Al-10 Ti	1.6	19.3	14	2.6	2.8

(1) —600 ℃ for 100 h; (2) —600 ℃ for 100 h + 630 ℃ for 150 h; φ_c —Calculated volume fraction; φ_e —Experimental volume fraction

Previous study revealed that the Al_3Ti particles in the RS Al-Ti alloy grew after a diffusion controlled process, obeying the LSW mechanism[9]. Low diffusivity (5×10^{-11} $m^2 s^{-1}$[10]) and equilibrium solubility (0.24 %[10]) of Ti in Al, as well as a relatively low boundary energy between Al_3Ti and the Al matrix guarantee good thermal stability of Al_3Ti particles, and hence excellent mechanical properties of Al-Ti alloys at elevated temperature. However, the LSW mechanism fails to explain the effects of the Ti concentration on the coarsening of particles since a very small volume fraction of the particles has been assumed. Actually, since the coarsening kinetics are controlled by the diffusion of solute from dissolving particles to growing particles, the mean separation between particles of a given average size decreases and the diffusion paths become shorter with increasing particle volume fraction of the Al-Ti alloy. Therefore, the coarsening rate of Al_3Ti particles increases with increasing Ti concentration, which results in larger Al_3Ti particles when thermal exposed under the same condition.

3.2 Elastic modulus

The elastic modulus of materials are of enginee-

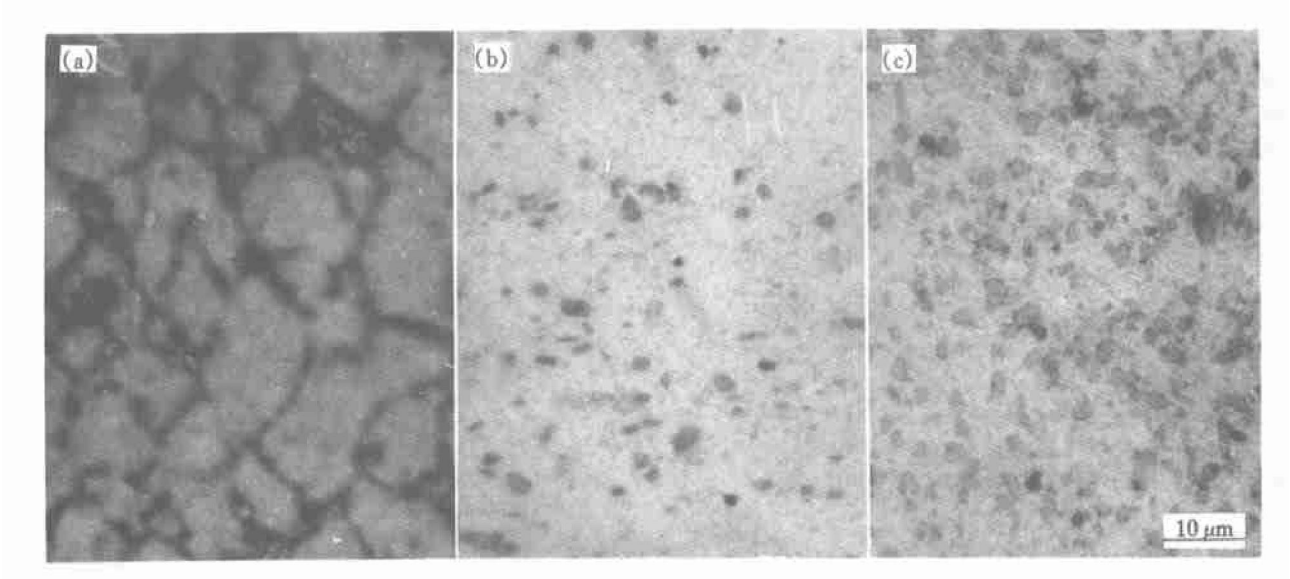

Fig.1 Microstructures of alloys after thermal exposure at 600 ℃ for 100 h

ring interest. Under external load, presence of reinforcers results in a heterogeneous disperse of stress in composites, which affects elastic modulus of the material. The following models have been used to evaluate the stiffness of composites

1) The mixing rule[11]:

$$E_c = E_f \varphi + E_m(1 - \varphi) \tag{1}$$

2) The Halpin-Tsai equation[11]:

$$E_c = E_m(1 + q\varphi)/(1 - q\varphi) \tag{2}$$

where

$$q = \left(\frac{E_f}{E_m} - 1\right)/\left(\frac{E_f}{E_m} + 1\right) \tag{3}$$

3) The modified shear lag (S-L) model[12]:

$$E_c = \varphi E_f\left[1 - \frac{(E_f - E_m^*)\,\mathrm{th}(ns)}{E_f ns}\right] + (1 - \varphi) E_m \tag{4}$$

where

$$E_m^* = \frac{1}{2}\{E_f[1 - \mathrm{sh}(ns)] + E_m\} \tag{5}$$

$$n = \{2E_m/[E_f(1 + \upsilon_m)\ln(R/r_0)]\}^{1/2} \tag{6}$$

r_0 is the radius of the fiber and R is the radius of the area around the fiber where the strain is homogeneous. Assuming that the fiber disperses hexagonally in the matrix, then $R/r_0 = 1/\sqrt{\varphi}$. s is aspect ratio of the particle. For the equiaxed particles, $s = 1$.

4) The Eshelby method[13]:

$$\boldsymbol{C}_c^{-1} = \boldsymbol{C}_m^{-1} - \varphi\{(\boldsymbol{C}_m - \boldsymbol{C}_f) \times [\boldsymbol{S} - \varphi(\boldsymbol{S} - \boldsymbol{I})] - \boldsymbol{C}_m\}^{-1}(\boldsymbol{C}_m - \boldsymbol{C}_f)\boldsymbol{C}_m^{-1} \tag{7}$$

$$E_c = E_{3c} = \frac{1}{\boldsymbol{C}_{3c}^{-1}} \tag{8}$$

where $\boldsymbol{C}_c$, $\boldsymbol{C}_f$ and $\boldsymbol{C}_m$ are stiffness matrices of the composite, reinforcer(fiber) and matrix, respectively. $\boldsymbol{S}$ is the Eshelby vector matrix and $\boldsymbol{I}$ is the identity matrix. Spherical particles are assumed in the calculation.

In the above mentioned equations, E_c, E_f and E_m refer to elastic modulus of the composite, reinforcer(fiber) and matrix, respectively. φ is the volume fraction of the reinforcers and υ_m is the Poison's ratio of the matrix.

For Al-Ti alloys, $E_m = 70$ GPa, $E_f = 220$ GPa, $\upsilon_m = 0.34$[14]. The elastic modulus predicted with the above mentioned models and the experiment results of the Al-Ti alloy with different particle volume fraction after thermal exposure at 600 ℃ for 100 h are listed in Table 2. It can be seen that the Halpin-Tsai equation and Eshelby method, which are considered excellent models applied to particle reinforced composites, have predicted the elastic modulus of the Al-Ti alloy quite well. The mixing rule, which provides an upper bound of the elasticity of composites, has given higher elastic modulus of the alloy. The modified shear lag model underestimated the elastic modulus of the alloy provided that the particle volume fraction exceeds 5%. The reason may be that, for spherical reinforcers, it is not appropriate to assume that the reinforcers disperse hexagonally in the matrix, then a revision of the definition of R/r_0 is provided. For the randomly distributed spherical particles with mean radius of r_0, the average center-to-center distance of R' between a particle and its nearest neighbor is[15]

Table 2 Elastic modulus of Al/Al_3Ti composition with different volume fraction of Al_3Ti

φ/ %	Elastic modulus/ GPa					
	exp	(1)	(2)	(3)	(4)	(5)
0.1	70.1	70.2	70.1	70.0	70.0	70.1
5	73.3	75.1	73.7	71.0	73.8	72.2
14	80.5	94.2	80.9	81.1	80.9	

(1) —Mixed rule; (2) —Halpin-Tsai equation; (3) —Modified shear lag model; (4) —Eshelby model; (5) —Re-modified shear lag model

$$R' = r_0\left(2 + \frac{\exp(8\varphi)\,\Gamma(\varphi)}{3\,\varphi^{1/3}}\right) \tag{9}$$

$$\Gamma(\varphi) = \int_{8\varphi}^{\infty} x^{-2/3}\exp(-x)\,\mathrm{d}x \tag{10}$$

It is reasonable to assume that $R = R'/2$. Therefore

$$R/r_0 = 1 + \frac{\exp(8\varphi)\,\Gamma(\varphi)}{6\,\varphi^{1/3}} \tag{11}$$

Using above equations, the calculation result of the modified S-L model coincides well with the experiment, as can be seen from Table 2 (Re-modified S-L).

WANG et al[16] obtained an increment of the elastic modulus of about 1.1 GPa for every 1% addition of Al_3Ti (volume fraction) in the Al-Ti alloy. Such a high increment is not achieved in our experiment.

3.3 Yield strength

The average tensile properties determined through three tests for each material are given in Table 3. The yield stress $\sigma_{0.2}$ and ultimate tensile stress σ_b increased with increasing volume fraction and decreasing particle size of the Al_3Ti particle, while the elongation δ increased at the reverse direc-

Table 3 Tensile properties of investigated materials

Alloy (mass fraction, %)	$\sigma_{0.2}$ / MPa	σ_b / MPa	δ / %	D / μm
Al-1.5Ti(1)	57	96.2	9.9	16
Al-1.5Ti(2)	53	95.8	9.9	19
Al-3.5Ti(1)	91	116.5	10	5.6
Al-3.5Ti(2)	85	112.5	9.9	6.2
Al-10Ti(1)	99	195.5	8.2	4.8
Al-10Ti(2)	93	191.8	8.5	5.1

Note: (1) —600 ℃ for 100 h; (2) —600 ℃ for 100 h + 630 ℃ for 150 h

tion.

Two kinds of strengthening mechanisms: the one based on load-sharing effects (the continuum mechanism) and the another based on dislocation movement, are developed to explain the improved strength of composites. In the former, parts of the applied load is supposed to transfer to the reinforcement through the interface between the reinforcer and the matrix, which improved the applied load to reach the yielding point of the matrix and hence improved the yield strength of the composite. The following modified shear lag model can be used to predict the yield strength of composites[17]

$$\sigma_c = \sigma_m[(s+2)\varphi + (1-\varphi)] \quad (12)$$

where σ_c and σ_m are yield strength of the composite and the matrix, respectively. Providing that $s=1$ for spherical Al_3Ti particles and taking the yield strength of the Al-1.5Ti alloy as the matrix yield strength ($\sigma_m = 55$ MPa), $\sigma_c = 56.4$ MPa and $\sigma_c = 58.9$ MPa are obtained for the Al-3.5Ti and the Al-10Ti alloy, respectively, which are far below the experimental values. Therefore, the mechanism based on load-sharing effects of the reinforcement fails to explain the improved yield strength of the Al-Ti alloy reinforced with Al_3Ti particles of 1.6 ~ 2.8 μm. This can be attributed to the fact that no further changes in the microstructure of the matrix have been considered. Furthermore, it is also noted that the effects of particle size on the yield strength of the Al-Ti alloy is not evident in the equation.

Various strengthening mechanisms based on dislocation movement theories have been considered in particle reinforced MMCs[18]:

1) quench strengthening, which results from the large difference in coefficient of thermal expansion between the reinforcers and the matrix (ΔC_t);

2) Orowan strengthening, which is negligible unless particles smaller than 1 μm are considered;

3) grain strengthening;

4) sub-structure strengthening;

5) work hardening.

It should be noted that opposite effects of the ΔC_t on the yield strength of composites exist. ΔC_t results in the generation of dislocations on quenching from the recrystallization or solution treatment temperature. The increased dislocation density contributes to the yield strength of the composite[19]. Conversely, ΔC_t also results in tensile stress in the matrix on quenching. The excess tensile stress decreases the yield strength of the composite[20]. In addition, ΔC_t between the Al_3Ti and Al is small[21]. Therefore, contributions of the quench strengthening are negligible provided that the particle size is larger than 1 μm. Contributions of the sub-structure strengthening can be ruled out since that the specimens have been annealed after cold rolling. Work hardening does not increase the yield strength significantly. Therefore, it may be concluded that the grain strengthening mechanism contributes mostly to the improvement of the yield strength of the Al-Ti alloy.

Since that the particle sizes of the reinforcers are all larger than 1 μm, and the RS Al-Ti alloy have been annealed at 500 ℃ for 1 h after cold rolling, the following equation based on recrystallization by particle stimulated nucleation (PSN) process can be used to predict the grain size of the Al matrix[18]:

$$D = d\left(\frac{1-\varphi}{\varphi}\right)^{1/3} \quad (13)$$

The calculation results are listed in Table 3 and further confirmed by OM and TEM observation. After thermal exposed at 600 ℃ for 100 h and followed by cold rolling and annealing, TEM observation revealed that the grain size of the aluminium matrix of Al-10Ti alloy is in the range of 4.5 ~ 5.0 μm, while that of Al-1.5Ti alloy is too large to be included in the view region of the TEM observation (as illustrated in Fig.2).

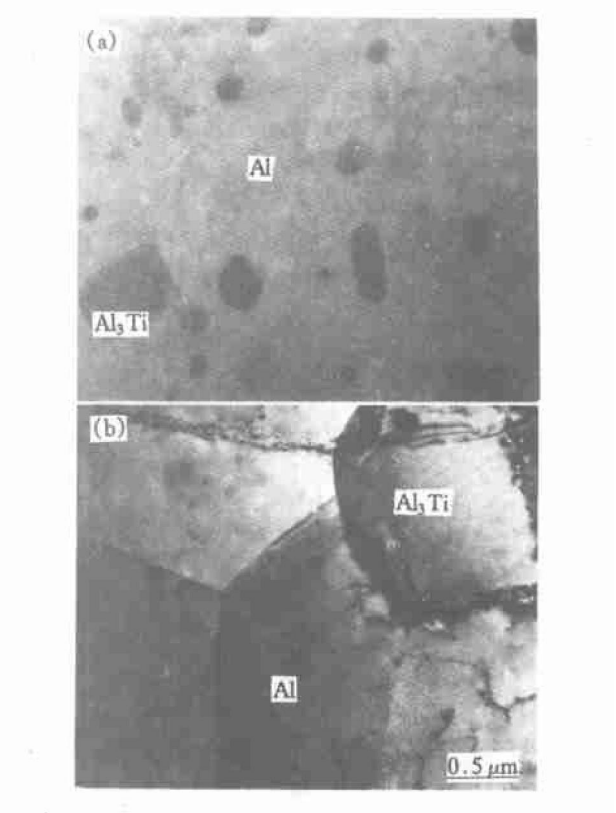

Fig.2 Microstructures of alloys after thermal exposed at 600 ℃ for 100 h
(a) —Al-1.5Ti; (b) —Al-10Ti

Fig.3 reveals the relationship between the yield stress $\sigma_{0.2}$ and $D^{-1/2}$ of Al-Ti alloys, which coincides quite well with the Hall-Petch equation

$$\sigma_{0.2} = \sigma_0 + k_y D^{-1/2} \quad (14)$$

This relationship indicates that the increased strength of Al-Ti alloys can be attributed predominantly to the fine grain of the matrix. The reinforce-

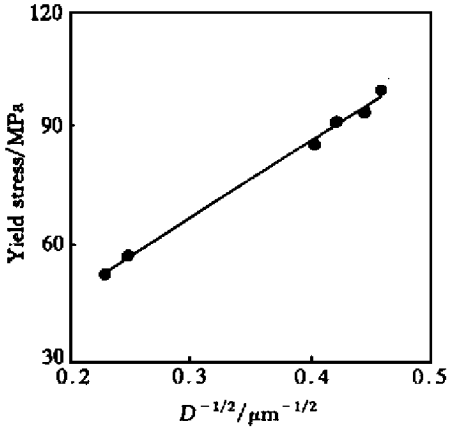

Fig .3 Relationship between yield stress $\sigma_{0.2}$ and $D^{-1/2}$ of Al-Ti alloy

ment particles with sizes of 1 .6 ~ 2 .8 μm contribute to the strength of the alloy through impeding grain growth of the matrix .

In addition , considering the low temperature yield strength of a dispersion hardened alloy , the strengthening effects of the dispersoid can be either the direct strengthening through interaction with dislocations (i .e . the Orowan strengthening) or the indirect strengthening through pinning the grain boundaries of the matrix[22] . If the direct and indirect hardening are designated as τ_d and τ_i, respectively , then

$$\frac{\tau_i}{\tau_d} = \frac{k_y}{Gb}\sqrt{\frac{\pi r}{2a}} \qquad (15)$$

where k_y is the constant of the Hall-Petch equation , G is the shear modulus of the material , b is the Burgers vector and r is the radius of the dispersoids , a is a constant . For Al-Ti alloy[20] , $k_y = 1.9 \times 10^5$ N• m$^{-3/2}$(Fig .3) , $Gb = 15$ N• m^{-1}[22] , $a = 1/4$[22] . Taking $r = 1.5 \times 10^{-6}$ m , then $\tau_i/\tau_d = 32.3$. The discrepancy between τ_d and τ_i provides another evidence that the main operative strengthening mechanism of the Al-Ti alloy is the fine grain strengthening .

Moreover , as indicated in Table 3 , the elongation of the alloy decreased from 9 .9 % to 8 .5 % when the volume fraction of the reinforcers of the alloy increased from 0 .1 % to 14 % . The minor decrease in the elongation can only be explained by the fine grain strengthening mechanism .

The fractographies in Fig .4 reveal the equiaxed dimples which are typical of ductile fracture . The density of dimples increased with increasing particle volume fraction , but not linearly . This suggests that microscopic crack does not necessarily nucleates at the interface between the particle and the matrix due to the strong Al_3Ti/Al bonding in the rapidly solidified Al-Ti alloy . In addition , it is found that fracture of the Al_3Ti particle is less likely to occur , as indicated in the high magnification morphology in Fig .4(c) .

4 CONCLUSIONS

1) After thermal exposure at a relatively high temperature for a long time , Al_3Ti particles in the rapidly solidified Al-Ti alloy coarsen to 1 .6 ~ 2 .8 μm . The coarsening rate increases with increasing nominal Ti concentration .

2) The elastic modulus of the Al-Ti alloy increases with increasing Al_3Ti particle volume fraction , which can be predicted using the Halpin-Tsai equation and Eshelby method . The generally used modified shear lag model is hereby re-modified to give a more precise evaluation of the elastic modulus of the particulate reinforced composite .

3) The yield stress $\sigma_{0.2}$ and ultimate tensile stress σ_b increase with increasing volume fraction

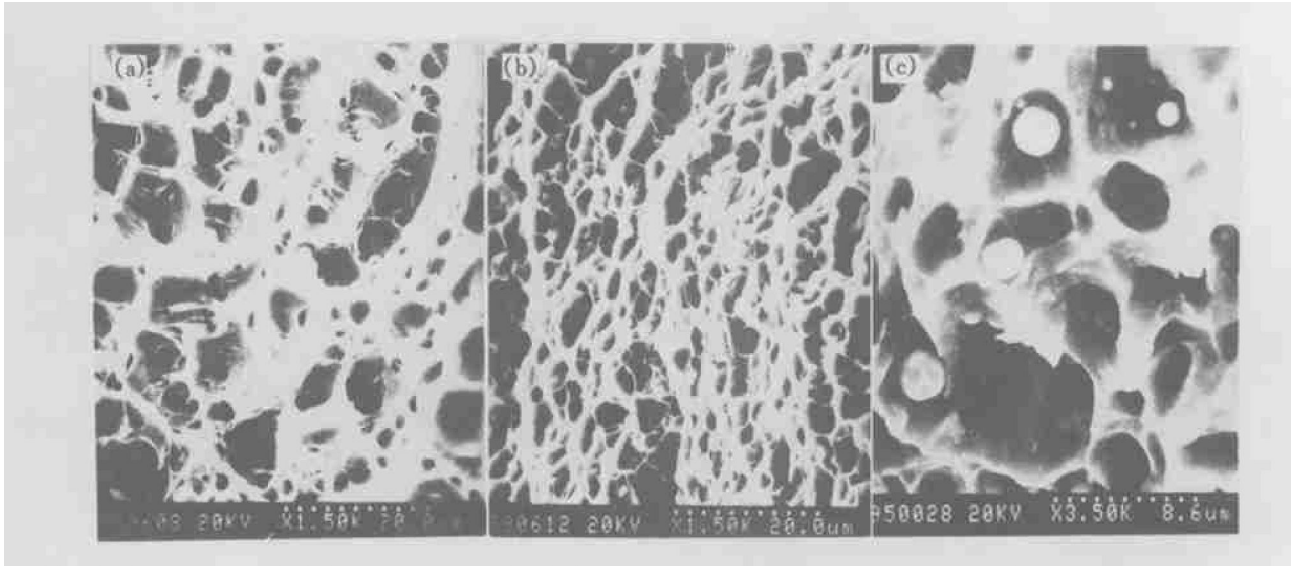

Fig .4 Mophologies of alloys after thermal exposure at 600 ℃ for 100 h + 630 ℃ for 150 h
(a) —Al-3 .5 Ti ; (b) ,(c) —Al-10 Ti

and decreasing particle size of the Al_3Ti particles. It is found that the main operative strengthening mechanism of the rapidly solidified Al-Ti alloy after thermal exposure is fine grain strengthening.

[REFERENCES]

[1] ZHANG X D and Loretto M H. Stability and decomposition mechanisms of supersaturated solid solutions in rapidly solidified aluminium-transition metal alloys [J]. Mater Sci Tech, 1996, 12(1): 19.

[2] Frazier W E and Koczak M J. Mechanical and thermal stability of powder metallurgy aluminum-titanium alloys [J]. Scr Metall, 1987, 21(2): 129.

[3] Lee K M and Moon I H. High temperature performance of dispersion-strengthened Al-Ti alloys prepared by mechanical alloying [J]. Mater Sci Eng, 1994, A185: 165.

[4] WANG S H, KAO P W and CHANG C P. Stress-strain behavior of fine-grained Al/AlTi alloys [J]. Acta Mater, 1993, 29(3): 323.

[5] Hideki Araki, Shigeoki Saji, Tsuyoshi Okabe, et al. Effect of pressure and temperature in consolidation of nanocrystalline MA powder of Al-10.7%Ti-0.6%Fe supersaturated solid solution [J]. Mater Trans JIM, 1997, 38(3): 247.

[6] Srinivasan S, Desch P B and Schwarz R B. Metastable phases in the Al_3X (X = Ti, Zr, and Hf) intermetallic system [J]. Scr Met Mater, 1991, 25: 2513.

[7] Nakamura M and Kimura K. Elastic constants of $TiAl_3$ and $ZrAl_3$ single crystals [J]. J Mater Sci, 1991, 26: 2208.

[8] Majumdar A and Muddle B C. Microstructure in rapidly solidified Al-Ti alloys [J]. Mater Sci Eng, 1993, 169(1): A135.

[9] WU N Q, WANG G X, LI Z Z, et al. Microstructure and sliding wear behavior of PM alloy Al-10Ti after thermal exposure [J]. Wear, 1997, 203: 155.

[10] MacCormack I B. Despersion strengthened P/M aluminium alloys [J]. Metals and Mater, 1986, 2(3): 131.

[11] Lloyd D J. Particle reinforced aluminum and magnesium matrix composites [J]. Int Mater Rev, 1994, 39(1): 1.

[12] Clyne T W. A simple development of shear lag theory appropriate for composites with a relatively small modulus mismatch [J]. Mater Sci Eng, 1989, A122: 183.

[13] Taya M and Arsenault R J. A comparison between a shear lay type model and an Eshelby type model in predicting the mechanical properties of a short fiber composite [J]. Scr Metall, 1987, 21(3): 349.

[14] Bernstein M L and Zaimovsky V A. Mechanical Properties of Metals [M]. (English translation), Moscow: Mir Publishers. 1983, 45.

[15] Ardell A J. The effect of volume fraction on particle coarsening: theoretical considerations [J]. Acta Metall, 1972, 20(1): 61.

[16] WANG S H and KAO P W. The strengthening effect of Al_3Ti in high temperature deformation of Al-Al_3Ti composites [J]. Acta Mater, 1998, 46(8): 2675.

[17] Nardone V C and Prewo K M. On the strength of discontinuous silicon carbide reinforced aluminum composite [J]. Scr Metall, 1986, 20(1): 43.

[18] Miller W S and Humphreys F J. Strengthening mechanisms in particulate metal matrix composites [J]. Scr Met Mater, 1991, 25(1): 33.

[19] Arsenault R J and Shi N. Dislocation generation due to difference between coefficients of thermal expansion [J]. Mater Sci Eng, 1986, 81: 175.

[20] Clyne T W and Withers P J. Introduction to Metal Matrix Composite [M]. (Chinese translation), Beijing: Metallurgical Industry Press. 1996, 70-76.

[21] Omura H, Miyoshi, Takahashi Y, et al. Dispersion Strengthened Aluminum alloys [M]. PA: TMS, Warrendale. 1998, 421-455.

[22] Hazzledine P M. Direct versus indirect dispersion hardening [J]. Scr Met Mater, 1992, 26(1): 57.

(Edited by LONG Huai-zhong)